Fadeyibi *et al.*
*Bulletin of the National Research Centre (2022) 46:190*
https://doi.org/10.1186/s42269-022-00882-1

Bulletin of the National Research Centre

RESEARCH Open Access

# Synthesis, characterization, and suitability of cocoyam starch-banana peels nanocomposite film for locust beans packaging

Adeshina Fadeyibi[1*], Kehinde Peter Alabi[1], Mary Fadeyibi[2] and Adewale Oluwaseun Adewara[1]

## Abstract

**Background:** Packaging of locust beans is done to prevent deterioration and promote its shelf-life. This research was carried out to develop and evaluate a cocoyam starch-banana peels nanocomposite film for locust beans packaging. The film was prepared by gelatinizing a mixture of 0.36 g banana peels nanoparticles (~ 1.14–1.64 nm), 18 g cocoyam starch, and 18 ml glycerol in 300 ml distilled water at 90 °C. The thermal, structural, mechanical and barrier properties of the film were determined using standard procedures. A 100 g of the locust beans condiment was packaged using the film and compared with packaging in a low-density polyethylene (LDPE) at 5.16–7.58 pH and 16.67–11.50% moisture ranges.

**Results:** Results indicate approx. 3% weight loss with an increase in temperature ($\leq$ 250 °C). The heat of decomposition in the process was 4.64 J/g, which depended on the transition temperature. Also, the film has high stiffness and creep along the line of topography in the atomic force imaging. The material permeates more to $CO_2$ (27%) and $H_2$ (67%) but has a low $O_2$ (4%) and $N_2$ (1%) gas permeabilities. The size of particles in the film was in the range of 3.52–3.92 nm, which is distributed across its matrix to create the pores needed to balance the gases in the microatmosphere. The microbial load of the locust beans decreased with pH and increased with moisture, but this was generally lower compared to those packaged in the LDPE at $p < 0.05$.

**Conclusions:** The film was a better packaging material than the LDPE since it recorded lower counts of the microbes throughout the storage. Thus, the nanocomposite film was effective in controlling the microbial growth of the locust beans irrespective of the sample moisture and pH over the 30 days packaging duration.

**Keywords:** Permeability, Thermal stability, Nanocomposite packaging, Microbial loads, Locust beans

## Background

Packaging is one of the crucial stages in food processing and preservation, which maintain the quality and prolong the shelf life of food products (Chawla et al. 2021; Ramos et al. 2018; Nasrollahzadeh et al. 2021). The packaging characteristics are dependent on the food product to be protected, so that different materials can be applied for different food products (Dogra et al. 2022; Atta et al. 2022). Traditionally, foods are packaged using the calabash, wooden boxes, immature palm fronds, plantain stem peels and dry cocoa leaves (Prajapati et al. 2021). These, however, can reduce the commercial value of the food since they cannot compete with modern packages in terms containerization and protection abilities (Gana Yisa et al. 2018). Thus, conventional materials are therefore needed for future food packaging applications.

Locust beans is a vegetable food that is consumed as seasoning in the diets in Nigeria. The preservation of the product is normally difficult because of its high perishability and the offensive odor it presents during

*Correspondence: adeshina.fadeyibi@kwasu.edu.ng

[1] Department of Food and Agricultural Engineering, Faculty of Engineering and Technology, Kwara State University, Malete, P.M.B. 1530, Ilorin, Kwara State, Nigeria
Full list of author information is available at the end of the article

processing. It is sometimes dried or marinated with salt to preserve it, but this procedure is often discouraged because of the quality decline it can cause (Sunmonu et al. 2020). The traditional packaging materials are also used to maintain the quality of the product, but this can cause market decline since the packages may not appeal to the consumers. Also, the product cannot compete with the conventional food seasoning such Maggi and Knor, because of poor packaging. However, the materials like the nylon are not suitable for locust beans packaging because they are not biodegradable and can constitute serious problem to the environment. An improved packaging technology that can address these challenges should effectively preserve the quality and extend the shelf-life of the locust beans.

Biodegradable packaging is an example of this technology, which can monitor and control the microsphere and therefore promote the shelf-life of the food. The material will normally help balance the concentration of gases by forming stable complexes that attenuate deterioration and maintain the quality of the packaged food (Chawla et al. 2021; Mousavi Khaneghah et al. 2018; Sharma et al. 2020). To achieve this, the biodegradable materials are incorporated with the nanoparticles to create a smart system with the desired properties. The resulting nanocomposite materials have been successfully used to package many types of food products. For instance, a cassava starch-zinc nanocomposite film has been successfully applied for tomatoes (Fadeyibi et al. 2017), okra slices (Fadeyibi et al. 2019a), cucumber, and garden eggs (Fadeyibi et al. 2020) packaging. However, the production of nanocomposite film from a blend cocoyam starch and banana peels nanoparticles has not been reported. Also, there is no available information on its practical or commercial application for the packaging of locust beans or any food product. Thus, the objectives of this research were to synthesize and characterize a nanocomposite film from the blend of the cocoyam starch and banana peels nanoparticles, and to evaluate its performance for the packaging of the locust beans at different pH and moisture contents.

## Methods

### Sources of materials

A kg each of cocoyam tubers (*Colocasia esculenta*) and unripe banana fruits (*Musa anamalu*) were purchased from Ipata market, Ilorin, Kwara State, Nigeria. All other materials used are listed in Table 1.

### Preparation of cocoyam starch

The cocoyam tubers were washed, peeled, and chopped into sizes, poured into a clean bowl, and then wet milled using a double disc attrition milling machine (Model SK-30-SS, NY) to form slurry. The slurry then sieved using a sieve, with a 150 μm mesh size, and allowed to settle for 24 h. The supernatant water was decanted, and the starch is placed in foiled aluminum trays and oven dried at a 70 °C for 18 h. The dried starch was then blended to obtain starch powder. The percentage yield of the starch in the cocoyam was 27.6%, and the proportion of amylose and amylopectin were 15.1% and 84.9%, respectively. The product was packed in an airtight container for further study.

### Preparation and particle size analysis of banana peels nanoparticles

Nanoparticles were prepared by processing the unripe banana fruits to remove the peels using a stainless-steel knife (13-inch Length) and washed with water to separate dirt. The material was cut into small pieces, dried in an oven at 50 °C for 48 h, and later grounded into fine powders using the blender (Model ISO14001 China). It was then subjected to sieve analysis using a mechanical sieve shaker (Model DSS200, Φ200mm, shaking freq. 221

**Table 1** List of materials for nanocomposite film development

| S/n | Materials | Information |
|---|---|---|
| 1 | Glycerol | 1000 ml analytical grade |
| 2 | Stainless steel knife | 13-Inch length |
| 3 | Sieve | Muslin cloth white |
| 4 | Acrylic sheet (plastic) | Size: 3 mm thickness, 4 × 4 feet |
| 5 | Plastic cutter | Blade dimension—width: 61 mm height: 19 mm |
| 6 | Plastic gum | Epoxy resin; hardener: dimethyldipropyltriamine |
| 7 | Disc attrition mill | Model SK-30-SS, NY |
| 8 | Mechanical sieve shaker | DSS200, Φ200mm, shaking freq. 221 times/min |
| 9 | Oven dryer | BS EN 61010-2-010:2003, Max. temp 250 °C |
| 10 | Blender | ISO14001 China, 110–120 V–60 Hz, 900 W |

times/min), which separates the particles to categories of various sizes. The fine samples collected at the pan was packed in an airtight polythene bag and stored in a desiccator for further study.

The size of the banana peels nanoparticles was determined using a UV-spectrophotometer (Model WSPECTRO-11003, Double beam, wavelength: 190–1100 nm) at the department of Food and Agricultural Engineering, Kwara State University, Malete. This was done by introducing a suspension of the fine particles into the machine and then allowing the UV light to incident on it. The amount of the light absorbed and transmitted were measured in the range of 495–700 nm wavelengths. The experiment was replicated three times, and the average values of the absorbance and transmittance of the particles were measured and recorded. The particle size of the nanoparticles was determined using Mie theorem, as reported by Doak et al. (2010). The theorem expresses the relationship between extinction efficiency, absorbance and the radius or particle size of a material (Eremin 2005), as shown in Eq. (1).

$$R = \left( \frac{Q_{ex}\lambda[(n_p + 2m)^2 + n_m^2}{24\pi^2 m^{1.5} n_m} \right)^{1/3} \quad (1)$$

$m$ is the relative refractive index of particle at $\lambda$; $n_p$ is the complex refractive index of the particle at $\lambda$; $n_m$ is the real refractive index of the particle at $\lambda$; $R$ is the particle size; $Q_{ex}$ is the extinction efficiency.

#### Preparation of nanocomposite film

Nanocomposite film was prepared by mixing 18 g of the cocoyam starch and 0.39 g of the nanoparticles with 300 ml of distilled water to form a paste based on trial evaluation and consistent with previous studies (Fadeyibi et al. 2017). This was followed by the addition of 18 ml of glycerol and heating in a burner for 20 min to form a thermoplastic solution. The solution was poured and allowed to spread out in a mold of 300 × 150 mm dimension and dried in an air circulated oven at 60 °C and relative humidity of 65% for 24 h.

#### Characterization of the nanocomposite film

The permeability of oxygen, carbon dioxide, nitrogen, hydrogen, and methane were determined by titration (Hadassah and Sehgal 2006), while water vapor permeability was determined using Karl Fischer's methodology (Kviesitis 1971). In the titration method, the carbon dioxide gas was passed through the film sample placed in a specially crafted lens mold, and the concentration of the released gas on the film was subsequently measured (Hadassah and Sehgal 2006). The exhaust gas was collected by dissolving in ethanol and the permeability to carbon dioxide was measured by titration of the solvent. The procedure was repeated for the hydrogen, nitrogen, methane, and oxygen gases. The experiment was repeated three times, and the average values of the measured gases were recorded as the gas permeability of the nanocomposite film. In Karl Fischer's method, the film sample was dissolved in an alcohol into a solution and then titrated against sulfur dioxide in the presence of a buffer (Schöffski and Strohm 2000). A solution of iodine was then added to the titration cell to oxidize the sulfur dioxide, and the amount of moisture absorbed by the film sample was analyzed (Schöffski and Strohm 2000). The experiment was repeated three times, and the mean amount of moisture measured was recorded as the water vapor permeability of the nanocomposite film.

The thermal properties of the nanocomposite film were determined using the thermogravimetric analyzer (TGA 55- TA Instrument) and a differential thermal analyzer (DTA) (Fadeyibi et al. 2017; Shanks 2010). In this method, the film was heated gradually and steadily to 600 °C in steps of 2 °C in a controlled nitrogen atmosphere. This results in weight degradation because of temperature exposure, and the resulting weight change was measured. The DTA provided information on the glass transition, crystallization, melting, and sublimation phase transformations occurring during the TGA analysis. The experiment was repeated three times, and the mean values of weight loss with the corresponding impact temperature, and processing energy were recorded as thermal property.

The microstructural property of the nanocomposite film was measured with the aid of scanning electron microscopy analysis (SEM, electron microscope model JEOL JSM-7600E) (Nikov et al. 2020). The analysis was done by subjecting the film sample to elemental composition analysis using an energy-dispersive X-ray spectroscopy (EDS) coupled to the SEM. This provides images of the physical structure showing the different constituents, elements, and their distribution. A further test was performed with the transmission electron microscope (TEM) to determine the size distribution and structural characteristics of the film material to 10, 20, and 50 nm resolutions.

The mechanical behavior of the nanocomposite film was analyzed using atomic force microscopy (AFM) (Muševič 2000; Eaton and West 2010). The AFM gives images of the mechanical characteristics of the film. In this method, a suspension of the film sample was prepared by dissolving it in ethanol with 0.1 mg/ml concentration and then indented at a rate of 0.5 μm/s under ambient temperature of 27 °C condition. A force–displacement curve was obtained by using a triangular shaped cantilever with the stiffness $k = 0.17$ N/m, made

with silicon nitride (Wright et al. 2010; Dhahri et al. 2013). To prevent stress concentration, a silicon dioxide spherical particle ($D=1$ μm) was attached at the end of the cantilever. The procedure was repeated three times, and the average values of displacement with corresponding force of indentation were recorded, as the mechanical properties of the nanocomposite film.

### Microbiological analysis of the packaged locust beans

A kg of African locust beans condiment was purchased from Malete main market, Kwara State, Nigeria, and used to evaluate the performance of the nanocomposite film. In this study, the moisture content and the pH of the locust beans condiment were varied by drying, using the air-circulated oven methods, in the range of 16.67–11.50% and 5.16–7.58, respectively. Thus, nine samples of the product, each weighing 100 g, were wrapped separately using the film, and another 100 g of the fresh sample was wrapped using the LDPE, which serves as the control experiment (Table 2). The packaged products were stored at ambient temperature of 27 °C, and the bacteria and fungi counts were determined at the end of 30 days storage, using standard methods (Sunmonu et al. 2020; Fadeyibi et al. 2017, 2019b, 2020). The experiment was replicated three times, and the average values of the microbial loads were recorded.

**Table 2** A layout of the variables for microbial load investigation

| Sample | Moisture content (%, wb) | pH |
|---|---|---|
| A | 16.67 | 7.58 |
| B | 13.33 | 7.58 |
| C | 11.50 | 7.58 |
| D | 16.67 | 6.66 |
| E | 13.33 | 6.66 |
| F | 11.50 | 6.66 |
| G | 16.67 | 5.16 |
| H | 13.33 | 5.16 |
| I | 11.50 | 5.16 |
| Control (LDPE) | 25.17 | 8.18 |

Letters A to I represent sample labels

### Statistical analysis

The data obtained from the barrier, mechanical, thermal, and structural characterizations were illustrated graphically. A Duncan multiple range test (DMRT) of the fungi and bacteria counts was carried out to compare the means among the film sample and with the LDPE sample at $p<0.05$ (Fadeyibi 2022), using an IBM SPSS Statistics Software (version 27.0.1.0). The data were replicated three times to reduce experimental error, and the average values and standard errors were determined.

## Results

### Size range characteristics of the banana peel nanoparticles

The result of the size range characterization of the nanoparticles is presented in Fig. 1. This was expressed as a plot of the wavelength versus absorbance in the UV light spectrum. Based on the analysis presented in the Mie theorem (Eq. 1), we obtained the particle size of the banana peel nanoparticles in the range of 3.48–4.92 nm between 495 and 700 nm wavelengths of the spectrum. The nanoparticles showed a negative response to heat absorbance but indicated a positive response to heat transmission at the various wavelengths.

### Barrier behavior of the nanocomposite film

The results of the barrier behavior of the nanocomposite film, which was used to package the locust beans condiment, is shown in Fig. 2. Based on the results presented

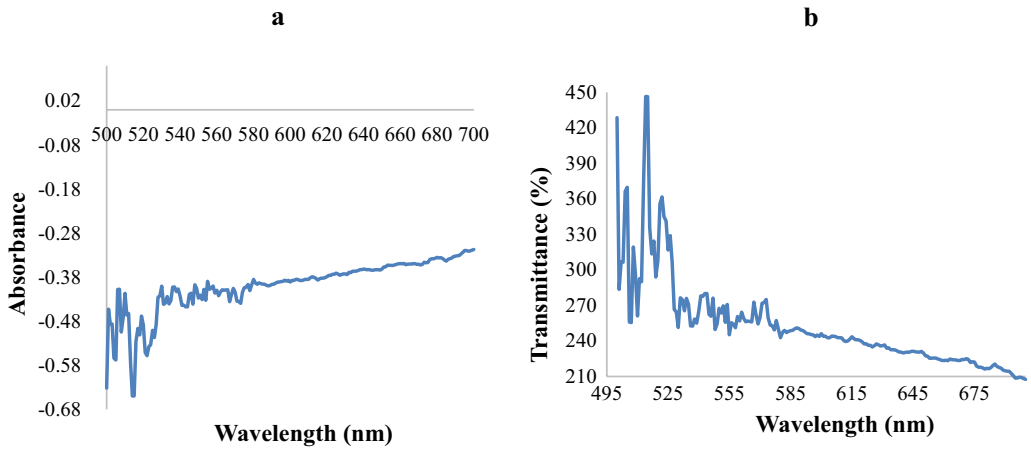


**Fig. 1** Effects of absorbance and transmittance of the banana peels nanoparticles

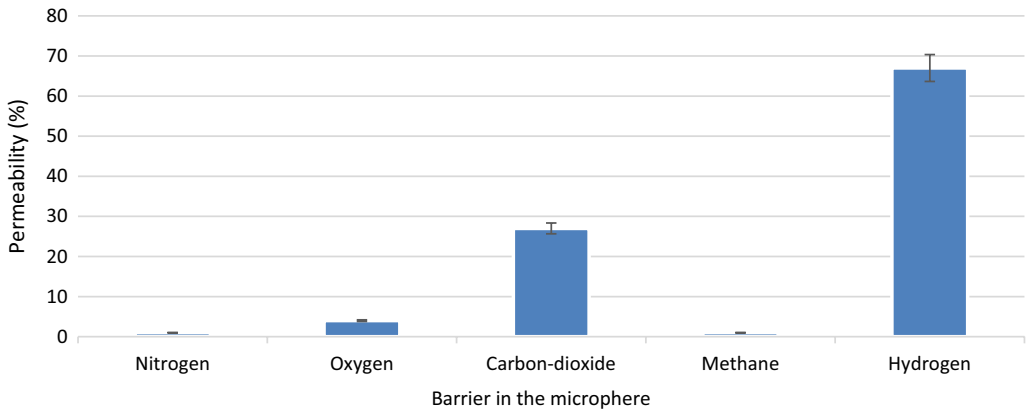


**Fig. 2** Permeability of the nanocomposite film

in Fig. 2, the nanocomposite film is an excellent material that can control the gas concentration (Mohammadpour and Naghib 2021) by allowing more carbon-dioxide (27%) and hydrogen (67%) gases, and less oxygen (4%) and nitrogen (1%) gases.

### Microstructural behavior of the nanocomposite film

The SEM micrographs of the nanocomposite film at different magnification ratios are shown in Fig. 3. This reveals some irregularities in shape and size by the appearance of voids within the matrix, thus indicating that the film contains heterogeneous particles. The TEM microtopography of the sample at vary temperature with a 3D picture of 10 nm, 20 nm, and 50 nm resolution of its microscopic properties is shown in Fig. 4.

### Thermal behavior of the nanocomposite film

The TGA/DTA results of the nanocomposite film is shown in Fig. 5. The weight lost increases with an increase in the temperature from 0 to 600 °C. At a threshold temperature of $\leq$ 250 °C, only approx. 3% weight of the nanocomposite film was degraded. The DTA results on the curve reveal that the phase transition of the film increase with temperature and the heat of decomposition was 4.64 J/g.

### Mechanical behavior of the nanocomposite film

The results of the AFM measurement of the nanocomposite film are shown in Fig. 6. A plot of the various forces and the film sample as a function of its mutual separation, which measures the stiffness of the film is also shown in Fig. 6. The indentation (δ) for the nanocomposite film is positive for the initial few nanometers' piezo displacement in the approach part of the force curve. However, due to the nonlinearity of the cantilever spring properties and AFM piezo's hysteresis, the indentation became negative in the last few nanometers piezo displacement at the end of the approach part of the force curve.

### Effect of moisture and pH on the microbial load of packaged locust beans

The mean comparison of the effect of moisture content and pH on the microbial loads of the packaged locust beans using the nanocomposite film and the LDPE is shown in Table 3. The film is a better packaging material than the LDPE since it records lower counts of the microbes throughout storage.

## Discussion

The absorption and transmission characteristics of molecules indicate the ability of the material to absorb and convey thermal energy in the packaging system (Hao et al. 2020). According to Goh et al. (Mohammadpour and Naghib 2021) and Pesika et al. (2003), a clear relation exists between the absorbance and particle size of nanoparticles. The authors reported an increase in the particle size of a zinc oxide nanoparticles with an increase in its absorbance. Also, a similar effect was reported by Doak et al. (2010) for the absorption spectra of gold nanoparticles. This property can be useful in the design of active food packaging material since they can assist in ensuring heat balance within the film's microsphere, that may otherwise cause food product deterioration.

Available literature has shown that perishable food products such as the locust beans typically produce oxygen, hydrogen, nitrogen, water vapor, carbon dioxide or methane during packaging (Kim et al. 2014; Ghosh and Singh 2022; Zhao et al. 2022). This can lead to a structural imbalance that can impact shelf life. Consequently, the gas concentration must be controlled so that the gases do not accumulate at destructive levels. This may create a stable microsphere, with high carbon dioxide and low

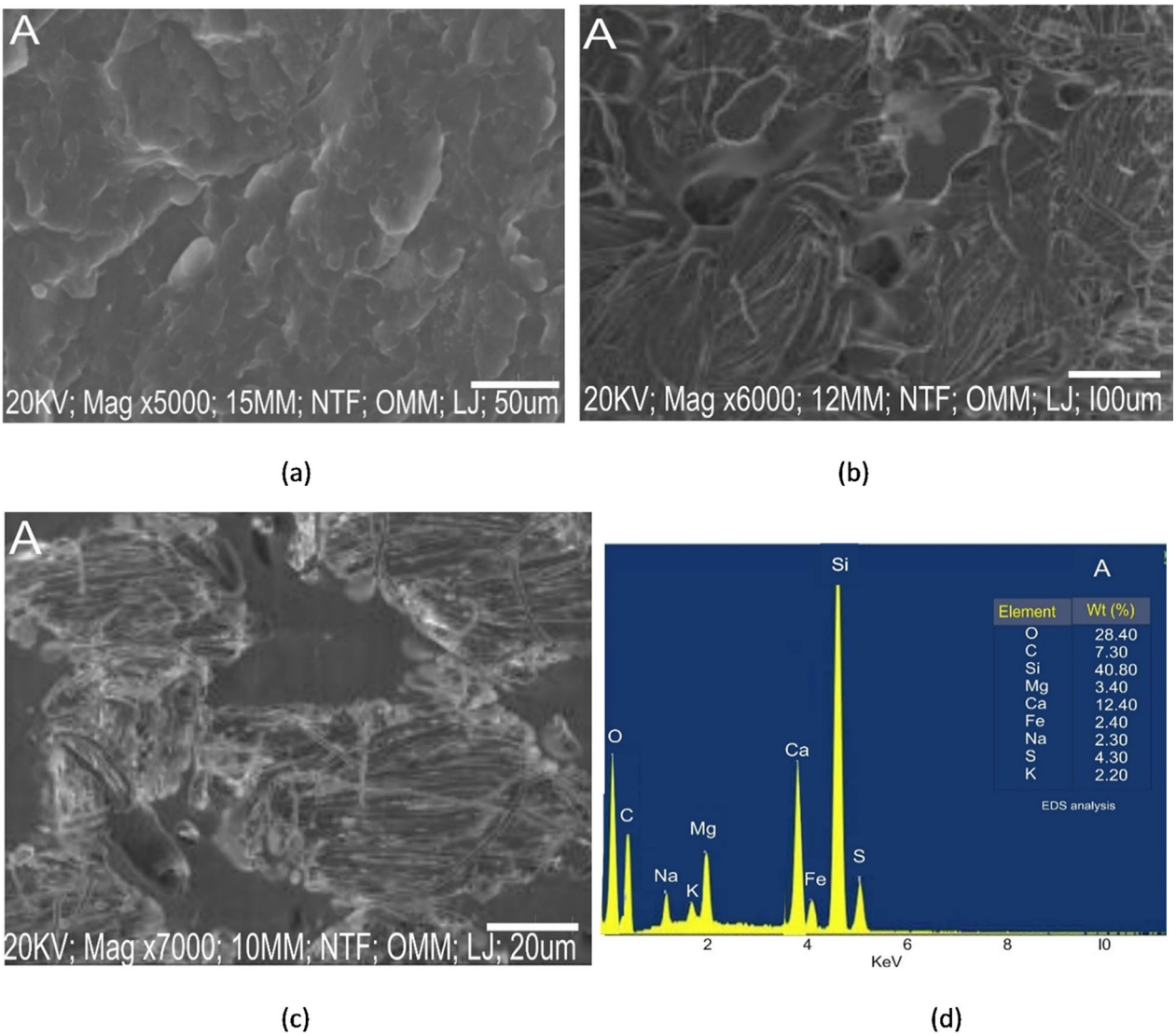


**Fig. 3** SEM micrographs of the nanocomposite film at different magnification ratios **a** 500, **b** 600, **c** 7000, **d** EDS analysis showing constituent elements

oxygen gases, which is beneficial for the packaging of the locust beans. As such, the product will experience anaerobic respiration, due to the small amount of oxygen gas available in the microsphere and raise the concentration of the carbon dioxide to promote its shelf life. This supports the findings by Zhang et al. (2020) who used graphene oxide nanosheets to promote the shelf-life of corn cellulose, and Zhang et al. (2020) who incorporated lignin in polyvinyl acetate to enhance the water vapor transmission rate of the film. In other related studies, Fadeyibi and Osunde (2021) incorporated a zinc nanoparticle in cassava starch, and Raja and Xavier (2021) functionalized a silane nanoparticle on nanoclay to enhance the keeping quality of the film during packaging. Therefore, based on the foregoing, the nanocomposite film can monitor and control the gas concentration in the microsphere during food packaging.

The size distribution extends around a narrow band of 500–700 nm, which, according to the Mie theorem (Hao et al. 2020; Goh et al. 2014), equates to 3.52–3.92 nm of particle size. Clearly, as expected, the size of the nanoparticles was less than the size of the matrix due to the presence of starch and glycerol molecules, which is spread over the film matrix to create the pores necessary to equilibrate the gases in the microsphere. The microstructural characterizations of Al–N nanocomposite film

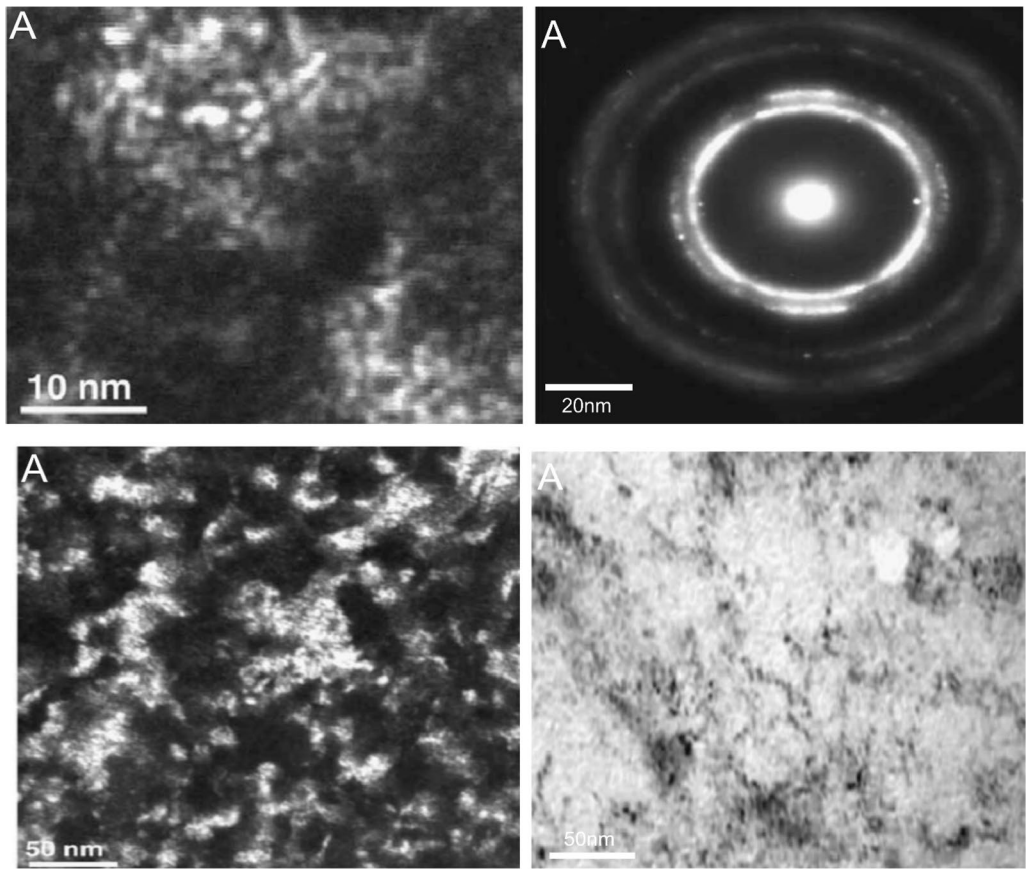


**Fig. 4** TEM microtopography showing the particle size and light permeability of the film

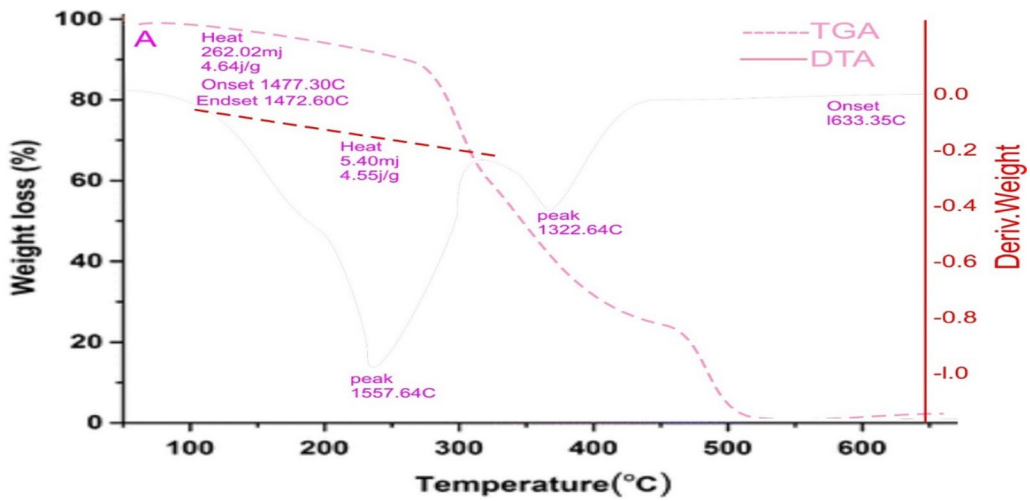


**Fig. 5** Effect of temperature on weight degradation of the nanocomposite film

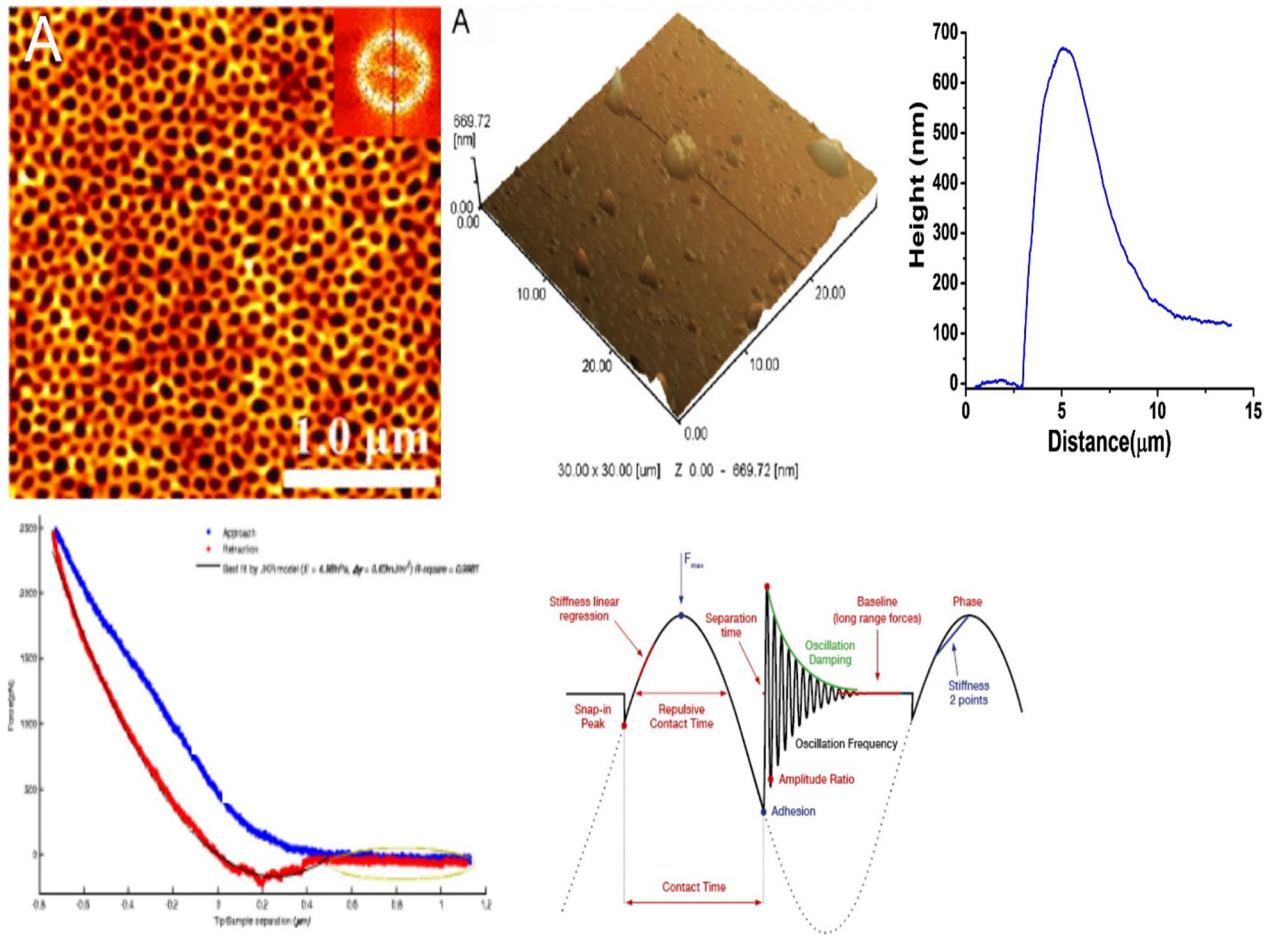


**Fig. 6** AFM showing the compactness of its molecules, its topography, and mechanical properties

**Table 3** Mean comparison among locust beans samples using the DMRT

| Sample | Fungi ($\times 10^3$ cfu/g) | Bacteria ($\times 10^3$ cfu/g) |
|---|---|---|
| Control (LDPE) | $2.30 \pm 0.007^{a}$ | $4.39 \pm 0.009^{a}$ |
| A | $1.19 \pm 0.007^{d}$ | $3.21 \pm 0.009^{b}$ |
| B | $1.14 \pm 0.007^{e}$ | $2.88 \pm 0.009^{c}$ |
| C | $1.11 \pm 0.007^{f}$ | $2.56 \pm 0.009^{d}$ |
| D | $1.21 \pm 0.007^{c}$ | $2.52 \pm 0.009^{e}$ |
| E | $0.09 \pm 0.007^{g}$ | $2.11 \pm 0.009^{f}$ |
| F | $0.08 \pm 0.007^{g}$ | $1.96 \pm 0.009^{g}$ |
| G | $1.32 \pm 0.007^{b}$ | $1.67 \pm 0.009^{h}$ |
| H | $1.14 \pm 0.007^{e}$ | $1.13 \pm 0.009^{i}$ |
| I | $0.86 \pm 0.007^{g}$ | $1.19 \pm 0.009^{j}$ |

Sample A to I retain their usual properties

Samples with the same letter number (a–j) are not significant at $p < 0.05$

(Li et al. 2018), $MoO_3$–$TiO_2$ nanocomposite film (Li et al. 2001), and ZnO–graphene oxide thin film nanocomposites film (Trinh et al. 2021) reported are related studies that support this finding. In addition, the EDS profile found in Fig. 3 denotes a strong silicon signal with low peaks in the potassium group. At the structural level, the nanocomposite film sample contains 40.80% (by weight) of the silicon compound and 2.20% (by weight) of the potassium compound. A similar result was reported by Nikov et al. (2020) in their work on the microstructural characterization of laser-ablated nanocomposites in a magnetic field. The physicochemical and microstructural properties of a polyvinyl alcohol mixed with a clay nanoparticle also did not reveal any obvious aggregation in the film matrix (Manikandan et al. 2019), nor did the film under study.

The images at 10 nm and 50 nm show a group of nanoparticles that congregate, and the location becomes darker. There are, however, a few parts showing white spots because of the lack of particles around them. The

dark spots may be caused by the presence of small particles, which have a high surface area, causing a high propensity for adhesion of the particles around the region (Manikandan et al. 2019). An appropriate view of defects causing particle size change may be seen at 50 nm. At 20 nm, the microstructural graphics display the presence of light permeability. This suggests that the film can have weak permeability to larger gas molecules.

The heat energy liberated during thermal heating of the film suggests 4.64 J of the heat energy needed to degrade only 1 g of the film sample within the glass transition or threshold temperature. The thermal stability of a green film based on the blend of poly (vinyl alcohol) and Eleusine *coracana composite film* (Manikandan et al. 2019), and blend of natural rubber and nano cellular whisker composite film (Thomas et al. 2021) are related studies that reported low weight degradation found below the glass transition temperature. Beyond the this, the film may not be suitable for packaging since a larger percentage of its weight was degraded and lost to excessive heating.

The cantilever displacement line does not overlap the piezo displacement line, thus resulting in significant depth of indentation for the retract part of the AFM force curve of the nanocomposite film. However, toward the end of the curve both the cantilever displacement line and piezo displacement line tends to meet and go along the same path showing equal amount of indentation. The AFM force curve for the nanocomposite film shows snap-in and snap-out due to the hydrophilicity of the material. Snap-in is a condition where the cantilever suddenly bends or is attracted to the sample due to the van der Waals attraction. After contact, the indenter will bend upward as it is continually pushed by the sample in the upward direction, thus increasing the contact force on the sample. During retraction, the indenter is initially prevented from separation due to adhesive forces which includes the van der Waals forces, the electrostatic force, capillary force, and the chemical bonds. At a certain distance of retraction, the indenter suddenly snaps out as the adhesive forces can no longer sustain the separation load.

Statistically, as shown in Table 3, there is significant difference in the number of bacteria counts between the samples packaged using the nanocomposite film and those packaged using the LDPE material at $p < 0.05$. Also, the fungi count in the samples E, F, and I are not significantly different from each other, but those in A to D and H are significantly different at $p < 0.05$. The observed difference can be associated with the presence of the nanoparticles in the film, which controlled the microbial activities and prevented their growth (Fadeyibi et al. 2017). Thus, the nanocomposite film was effective in controlling the microbial growth irrespective of the sample moisture and pH over the 30 days duration of packaging. In related studies, the performance starch blended with zinc nanocomposite film has been reported for tomatoes (Fadeyibi et al. 2017), okra slices (Fadeyibi et al. 2019a), and cucumber (Fadeyibi et al. 2020) preservations. This means that the film has antimicrobial abilities, just like other similar films, to control the growth of the microorganisms during food preservation.

## Conclusions

A novel nanocomposite packaging material was synthesized from the blend of banana peels nanoparticles and cocoyam starch and evaluated for locust beans packaging. The results showed that the size of the nanoparticles was in the range of 1.14–1.64 nm. Also, the film permeability was high for the carbon-dioxide (27%) and hydrogen (67%) gases, and low for the oxygen (4%) and nitrogen (1%) gases within the microsphere. This means that it can control the gas concentration by allowing more carbon-dioxide and low oxygen concentration within the system. The size distribution in the film matrix ranges around a narrow band length of 500–700 nm, which corresponds to 3.52–3.92 nm particle size range. At a threshold temperature of $\leq 250$ °C, only approx. 3% weight of the nanocomposite film was degraded. The DTA results on the curve reveal that the phase transition of the film increase with the temperature and the heat of decomposition in the process was 4.64 J/g. This means 4.64 J of the heat energy was required to degrade only 1 g of the film sample within the glass transition or threshold temperature. The film was a better packaging material than the LDPE since it recorded lower counts of the microbes throughout the storage. There is a significant difference between the microbial loads in the individual sample and their interaction at $p < 0.05$. Thus, the nanocomposite film was effective in controlling the microbial growth of the locust beans irrespective of the sample moisture and pH over the 30 days packaging duration.

#### Abbreviations

m: Relative refractive index of particle at $\lambda$; $n_p$: Complex refractive index of the particle at $\lambda$; $n_m$: Real refractive index of the particle at $\lambda$; R: Particle size; $Q_{ex}$: Extinction efficiency; k: Stiffness; Φ: Diameter; DTA: Differential thermal analyzer; TGA: Thermogravimetric analyzer; SEM: Scanning electron microscope; EDS: Energy-dispersive X-ray spectroscopy; TEM: Transmission electron microscope; AFM: Atomic force microscopy; LDPE: Low density polyethylene; ANOVA: Analysis of variance; UV: Ultraviolet radiation; Al–N: Aluminum nitrogen; $MoO_3$–$TiO_2$: Molybdenum trioxide–titanium dioxide.

#### Acknowledgements

The authors acknowledge the technical assistance provided by the Laboratory staff in the department of Food and Agricultural Engineering, Kwara State University Malete, Nigeria.

**Author contributions**
AF conceived the idea, designed the experiment, performed the SEM and TGA study on the film, wrote the initial draft, and edited the final manuscript. KPA performed AFM study on the film and interpreted the data. MF performed the microbiological study on the packaged product and interpreted the data statistically. AOA synthesized the nanocomposite film, performed permeability test on the film and conducted literature review. All authors have read and approved the final manuscript.

**Funding**
There is no funding available for this publication.

**Availability of data and materials**
Data and materials will be made available on request.

## Declarations

**Ethics approval and consent to participate**
Not applicable.

**Consent for publication**
Not applicable.

**Competing interests**
The authors declare no competing interests.

**Author details**
[1]Department of Food and Agricultural Engineering, Faculty of Engineering and Technology, Kwara State University, Malete, P.M.B. 1530, Ilorin, Kwara State, Nigeria. [2]Department of Biological Sciences, Faculty of Science, Augustine University, Ilara-Epe, P.M.B 1010, Epe, Lagos State, Nigeria.

Received: 4 March 2022 Accepted: 25 June 2022
Published online: 01 July 2022

**References**

Atta OM, Manan S, Shahzad A et al (2022) Biobased materials for active food packaging: a review. Food Hydrocoll 125:107419. https://doi.org/10.1016/J.FOODHYD.2021.107419
Chawla R, Sivakumar S, Kaur H (2021) Antimicrobial edible films in food packaging: current scenario and recent nanotechnological advancements—a review. Carbohydr Polym Technol Appl 2:100024. https://doi.org/10.1016/J.CARPTA.2020.100024
Dhahri S, Ramonda M, Marlière C (2013) In-situ determination of the mechanical properties of gliding or non-motile bacteria by atomic force microscopy under physiological conditions without immobilization. PLoS ONE. https://doi.org/10.1371/JOURNAL.PONE.0061663
Doak J, Gupta RK, Manivannan K et al (2010) Effect of particle size distributions on absorbance spectra of gold nanoparticles. Physica E 42:1605–1609. https://doi.org/10.1016/J.PHYSE.2010.01.004
Dogra V, Verma D, Fortunati E (2022) Biopolymers and nanomaterials in food packaging and applications. Nanotechnol-Based Sustain Altern Manag Plant Dis. https://doi.org/10.1016/B978-0-12-823394-8.00011-1
Eaton P, West P (2010) Atomic force microscopy. atomic force. Microscopy 9780199570454:1–256. https://doi.org/10.1093/ACPROF:OSO/9780199570454.001.0001
Eremin YA (2005) SCATTERING | scattering theory. In: Encyclopedia of Modern optics, five-volume set, pp 326–330. https://doi.org/10.1016/B0-12-369395-0/00682-5
Fadeyibi A (2022) Modeling rheological behavior of beef based on time-dependent deformation and packaging. Gazi Univ J Sci 34:997–1008. https://doi.org/10.35378/gujs.742087
Fadeyibi A, Osunde ZD (2021) Effect of thickness and matrix variability on properties of a starch-based nanocomposite supple film. Food Res 5:416–422. https://doi.org/10.26656/FR.2017.5(4).281
Fadeyibi A, Osunde ZD, Egwim EC, Idah PA (2017) Performance evaluation of cassava starch-zinc nanocomposite film for tomatoes packaging. J Agric Eng 48:137–146. https://doi.org/10.4081/JAE.2017.565
Fadeyibi A, Osunde A, Yisa MG (2019a) Optimization of processing parameters of nanocomposite film for fresh sliced okra packaging. J Appl Packag Res 11:1–10
Fadeyibi A, Osunde ZD, Yisa MG (2019b) Prediction of some physical attributes of cassava starch-zinc nanocomposite film for food-packaging applications. J Packag Technol Res 3:35–41. https://doi.org/10.1007/S41783-018-0046-1
Fadeyibi A, Osunde Z, Yisa MG (2020) Effects of period and temperature on quality and shelf-life of cucumber and garden-eggs packaged using cassava starch-zinc nanocomposite film. J Appl Packag Res 12:1–10
Gana Yisa M, Fadeyibi A, Abdul Hafe S (2018) Design, fabrication and testing of a manually operated locust bean cubing machine. Asian J Appl Sci 11:56–63. https://doi.org/10.3923/AJAPS.2018.56.63
Ghosh M, Singh AK (2022) Potential of engineered nanostructured biopolymer based coatings for perishable fruits with Coronavirus safety perspectives. Prog Org Coat. https://doi.org/10.1016/J.PORGCOAT.2021.106632
Goh EG, Xu X, McCormick PG (2014) Effect of particle size on the UV absorbance of zinc oxide nanoparticles. Scr Mater 78–79:49–52. https://doi.org/10.1016/J.SCRIPTAMAT.2014.01.033
Hadassah J, Sehgal PK (2006) A novel method to measure oxygen permeability and transmissibility of contact lenses. Clin Exp Optom 89:374–380. https://doi.org/10.1111/J.1444-0938.2006.00080.X
Hao X, Hou W, Shi Z, Fan C (2020) Sensitivity study of synthetic polarization measurements in UV wavelength bands, vol 19. https://doi.org/10.1117/12.2579307
Kim HJ, Kim SJ, An DS, Lee DS (2014) Monitoring and modelling of headspace-gas concentration changes for shelf life control of a glass packaged perishable food. LWT Food Sci Technol 55:685–689. https://doi.org/10.1016/J.LWT.2013.10.018
Kviesitis B (1971) Determination of water in molasses by Karl Fischer method. J AOAC Int 54:1231–1235. https://doi.org/10.1093/JAOAC/54.5.1231
Li YX, Galatsis K, Wlodarski W et al (2001) Microstructural characterization of MoO3-TiO2 nanocomposite thin films for gas sensing. Sens Actuat B Chem 77:27–34. https://doi.org/10.1016/S0925-4005(01)00668-2
Li W, Zhang K, Liu P et al (2018) Microstructural characterization and strengthening mechanism of AlN/Y nanocomposite and nanomultilayered films. J Alloy Compd 732:414–421. https://doi.org/10.1016/J.JALLCOM.2017.10.244
Manikandan KM, Yelilarasi A, Senthamaraikannan P et al (2019) A green-nanocomposite film based on poly(vinyl alcohol)/Eleusine coracana: structural, thermal, and morphological properties. Int J Polym Anal Charact 24:257–265. https://doi.org/10.1080/1023666X.2019.1567087
Mohammadpour Z, Naghib SM (2021) Smart nanosensors for intelligent packaging. Nanosens Smart Manuf. https://doi.org/10.1016/B978-0-12-823358-0.00017-4
Mousavi Khaneghah A, Hashemi SMB, Limbo S (2018) Antimicrobial agents and packaging systems in antimicrobial active food packaging: an overview of approaches and interactions. Food Bioprod Process 111:1–19. https://doi.org/10.1016/J.FBP.2018.05.001
Muševič I (2000) Atomic force microscopy. Inf MIDEM 30:223–227. https://doi.org/10.1093/OSO/9780198856559.003.0016
Nasrollahzadeh M, Nezafat Z, Shafiei N, Bidgoli NSS (2021) Food packaging applications of biopolymer-based (nano)materials. Biopolym-Based Met Nanoparticle Chem Sustain Appl. https://doi.org/10.1016/B978-0-323-89970-3.00004-4
Nikov R, Avdeev G, Dikovska A et al (2020) Microstructural characterization of nanocomposites produced by laser ablation in a magnetic field. J Phys: Conf Ser. https://doi.org/10.1088/1742-6596/1492/1/012057
Pesika NS, Stebe KJ, Searson PC (2003) Relationship between absorbance spectra and particle size distributions for quantum-sized nanocrystals. J Phys Chem B 107:10412–10415. https://doi.org/10.1021/JP0303218
Prajapati VD, Maheriya PM, Roy SD (2021) Locust bean gum-derived hydrogels. Plant Algal Hydrogels Drug Deliv Regen Med. https://doi.org/10.1016/B978-0-12-821649-1.00016-7
Raja Beryl J, Xavier JR (2021) Influence of silane functionalized nanoclay on the barrier, mechanical and hydrophobic properties by clay nanocomposite films in an aggressive chloride medium. Colloids Surf A. https://doi.org/10.1016/J.COLSURFA.2021.127625
Ramos ÓL, Pereira RN, Cerqueira MA et al (2018) Bio-based nanocomposites for food packaging and their effect in food quality and safety. Food Packag Preserv. https://doi.org/10.1016/B978-0-12-811516-9.00008-7

Schöffski K, Strohm D (2000) Karl Fischer moisture determination. Encycl Anal Chem. https://doi.org/10.1002/9780470027318.A8102
Shanks RA (2010) Thermal characterization of nanocomposites. Recent Adv Polym Nanocompos Synth Charact. https://doi.org/10.1163/EJ.9789004172975.I-438.107
Sharma R, Jafari SM, Sharma S (2020) Antimicrobial bio-nanocomposites and their potential applications in food packaging. Food Control. https://doi.org/10.1016/J.FOODCONT.2020.107086
Sunmonu M, Fadeyibi A, Olabanjo O (2020) Moringa ve farklı depolama malzemeleri kullanarak toz Irvingia gabonensis'in kalitesi ve mikrobiyal inaktivasyonu. Harran Tarım ve Gıda Bilim Derg. https://doi.org/10.29050/HARRANZIRAAT.733598
Thomas SK, Dileep P, Begum PMS (2021) Green polymer nanocomposites based on natural rubber and nanocellulose whiskers from Acacia caesia: Mechanical, thermal, and diffusion properties. Mater Today Proc. https://doi.org/10.1016/J.MATPR.2021.11.613
Trinh TQ, Nguyen TT, Vu DV, Le DH (2021) Microstructural analysis and thermoelectric performance of Ga-doped ZnO/reduced graphene oxide thin film nanocomposites. Ceram Int 47:32033–32042. https://doi.org/10.1016/J.CERAMINT.2021.08.092
Wright CJ, Shah MK, Powell LC, Armstrong I (2010) Application of AFM from microbial cell to biofilm. Scanning 32:134–149. https://doi.org/10.1002/SCA.20193
Zhang X, Liu W, Liu W, Qiu X (2020) High performance PVA/lignin nanocomposite films with excellent water vapor barrier and UV-shielding properties. Int J Biol Macromol 142:551–558. https://doi.org/10.1016/J.IJBIOMAC.2019.09.129
Zhao M, Zhang Z, Cai H et al (2022) Controlled moisture permeability of thermoplastic starch/polylactic acid/poly butylene adipate-co-terephthalate film for the autolysis of straw mushroom Volvariella volvacea. Food Chem. https://doi.org/10.1016/J.FOODCHEM.2021.131409

## Publisher's Note